White Rose
university consortium
Universities of Leeds, Sheffield & York

Modelling aqueous corrosion of nuclear waste phosphate glass

Pavel P. Poluektov[a], Olga V. Schmidt[a], Vladimir A. Kascheev[a], Michael I. Ojovan[b1]

[a]Bochvar All-Russian Scientific Research Institute for Inorganic Materials (VNIINM), Moscow, Russia
[b]Immobilisation Science Laboratory, Department of Materials Science and Engineering, University of Sheffield, Mappin Street, Sheffield, S1 3JD, United Kingdom,
Tel.: +44 747 828 9098, e-mail: m.ojovan@sheffield.ac.uk

Abstract

A model is presented on nuclear sodium alumina phosphate (NAP) glass aqueous corrosion accounting for dissolution of radioactive glass and formation of corrosion products surface layer on the glass contacting ground water of a disposal environment. Modelling is used to process available experimental data demonstrating the generic inhibiting role of corrosion products on the NAP glass surface.

Keywords: Nuclear waste, Phosphate glass, Corrosion, Modelling, Long-term durability

1. Introduction

High-level radioactive waste (HLW) with typical specific activity above 10^{10} Bq/L is currently generated by water-extraction processing of irradiated e.g. spent or used nuclear fuel (SNF or UNF) typically in form of aqueous nitrate solutions [1-5]. Vitrification is used on industrial scale for immobilization of this waste in a vitreous (glassy) wasteform. Sodium-alumina-phosphate (NAP) glasses are widely used for this purpose in Russia whereas western countries (UK, France, Belgium, Germany), USA, Japan, India and China use boron-silicate (BS) glasses [6-11]. The justification on using NAP glasses lays upon composition of Russian HLW containing large amounts of aluminium oxide. Additional arguments on selecting NAP glasses were the relatively low melting (processing) temperature (900 ÷ 1050 $^{\circ}$C), liquid-feeding and easy of dosage systems. Indeed the NAP glass is particularly attractive for immobilisation of wastes containing large amounts of Al and Na. In contrast to BS glasses phosphate glasses incorporate significantly larger amounts of corrosion products as well as actinide oxides, molybdates and sulphates. Lanthanides and actinides in phosphate glasses tend to complex strongly with phosphate ions. Fig. 1 shows the glass forming regions of the Na_2O-Al_2O_3-P_2O_5 system with data on solubility of some HLW components in melted phosphate glass at 1000°C given in [4, 10].
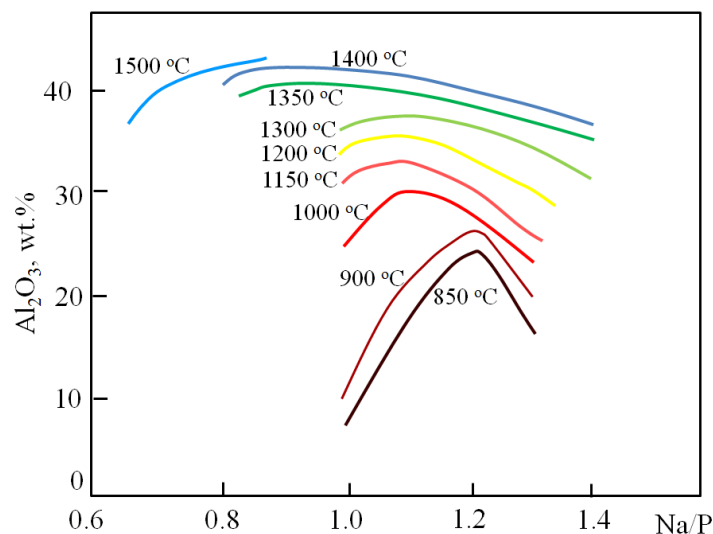

Fig. 1. Mass content of Al_2O_3 as a function of (Na/P) ratio at constant temperatures for NAP glasses (Na_2O-Al_2O_3-P_2O_5).

---

[1] Corresponding author

The optimum range of the Na to P ratio is from 1.0 to 1.3 for low (850 – 950 ºC) to moderate (1200 – 1300 ºC) melting temperatures of glass processing. This ratio can be increased at higher temperatures: NAP glasses can contain up to 40% Al_2O_3 at 1400-1500 °C.

Four generations of EP-500 direct (joule) heating melters for waste vitrification have been operating at PO "Mayak" since 1987 [9, 10]. The vitrification facilities have produced since then 6,200 tonnes of radioactive glass totalling 643 MCi (23.79 YBq) [6, 7, 12]. The molten radioactive glass is poured from the melter into 200 L cans made of mild steel. These cans are then collected into cases containing 3 cans each and further stored in a dedicated storage facility until the final disposal site will be available. The storage facility is now filled above 90% of its design capacity. Currently the fifth generation of EP-500 melter and a new vitrified HLW storage facility are under construction. The storage facility will be operational during the next 40 years after that the vitrified HLW will be disposed of in a geological disposal facility. Disposal of vitrified HLW shall ensure its safety for the entire period of radionuclides decay e.g. for the geological timescales of many hundred thousands of years [3, 4, 13-18]. Although the safety requirements belong to the waste package disposed of the role of glassy wasteform as the primary barrier is crucial in ensuring the overall safety of transportation, storage and disposal.

Vitrified HLW in a disposal environment could eventually at a later stage of disposal after some thousand years contact groundwater although there is small likelihood that the contact can occur at earlier stages due to low probability destructive events. On contacting water the glass corrodes with main two types of radionuclide release being hydrolysis and diffusion-controlled ion exchange. With time the dominant corrosion process is glass hydrolysis when glass constituents are dissolved of and removed with water and a gel-like product forms on the surface (see the reviews [19-22]). Sodium- and phosphate-ions are the relatively mobile components of NAP glasses whereas aluminium hydroxide and non-soluble phosphates form the corrosion layer on glass surface [10]. The porosity of latter determines its transport capabilities of water-dissolved glass components. The structure of corrosion layer can change with time and that changes its permeability. For example the interaction of matter dissolved with non-dissolved precipitate in the pores can clog them and thus block the pathways of solution leading to a lower corrosion rate.

Corrosion of glass is widely investigated [19-30] although there is not yet a generically accepted understanding of that process on geological disposal of radioactive waste. This in its turn leads to an absence of generically accepted permitted levels of radioactive glass corrosion. Because of that the interest to glass corrosion is not diminishing including methodology for investigation of process and its modelling [31].Long-term durability models are still being refined with international efforts on a refined understanding glass corrosion mechanism [19, 31]. In this work we propose a mathematical model of NAP glass corrosion in aqueous solutions relevant to geological disposal. The model accounts for leaching (dissolution) of glass components and formation of corrosion layers on the glass surface and transport of these components through the corrosion layer. The equations obtained are then used to model experimental data from available published sources.

The composition of NAP glass used in Russia to immobilise HLW is represented on oxide basis in wt.% by alkali oxides amounting 24 – 27, aluminium and other multivalent metal oxides 20 – 24 and phosphorus oxide 50 – 52 [4, 10]. Durability of glasses in an aqueous environment strongly depends on many parameters such as temperature, solution pH and composition, water flow rate etc. Leaching rate of radionuclides is determined by the rate of glass corrosion and interaction of corrosion products with chemical species of groundwater. The composition of latter is determined by interaction of water with geological formation and materials present or formed in the disposal facility for example resulting from corrosion of containers. We present here data on NAP glass corrosion and its components leaching via a mathematical model of physical and chemical destruction of radioactive glass and formation of surface layer on the glass contacting ground water. The latter is controlling the transport of species between the glass and ground water. Modelling is then used to process available experimental data from [32].

2. NAP glass corrosion in disposal conditions

To characterise processes that occur on NAP glass contacting ground water it is necessary to determine the glass components that are transferred to water and their form in the solution as well as their interaction with species in water. Fig. 2 shows schematically corrosion processes in a closed aqueous system similar to that characteristic of a typical geological disposal system when the water exchange rate is extremely small or ideally nil. Note that in opposite conditions of fast flowing water the corrosion processes show a distinct initial diffusion-controlled ion exchange corrosion mechanism followed by a hydrolysis-controlled corrosion process [4, 33, 34].
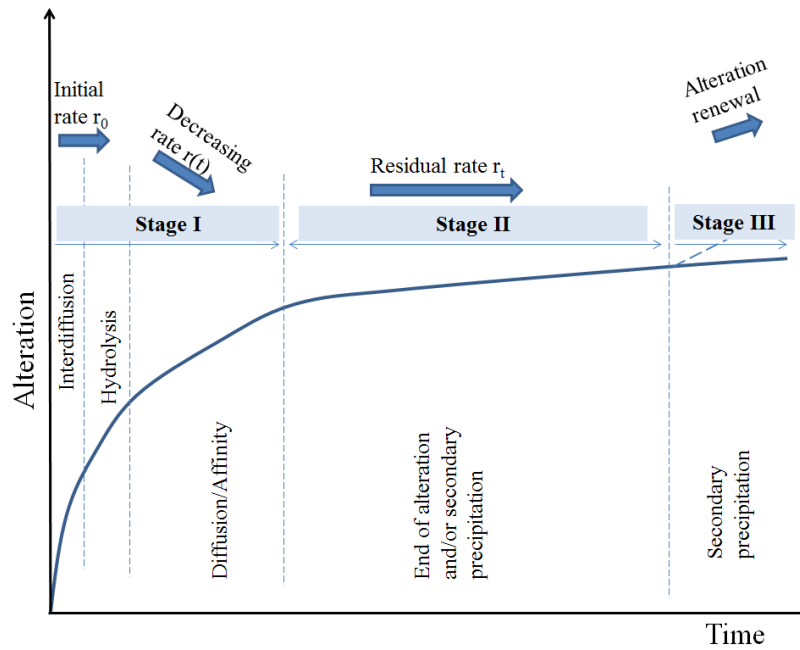
Fig. 2. Schematic of glass corrosion processes in typical geological disposal conditions.

Three distinct phases of glass corrosion are revealed depending of glass corrosion mechanisms which are characterised as follows [22, 35]:

- Stage I of glass dissolution encompasses zones where multiple mechanisms are operative including regimes that are ion exchange interdiffusion-controlled, hydrolysis-controlled, and a rate drop that is diffusion or affinity controlled.
- Stage II of glass dissolution characterised by a steady state or residual rate signals the end of the alteration phase and/or a pseudo-equilibrium between the alteration and re-condensation reactions.
- Stage III of glass dissolution is characterised by resumption of alteration with a return to a forward rate.

Glass corrodes rapidly during the Stage I because the glass is in contact with fresh groundwater solution containing little of glass components. During this stage there is an exchange between solution species (H_2O, O, H_3O, etc.) and glass (alkali, phosphorus, alkali earths, etc.). Apart from that due to hydrolysis a part of bound phosphorus transforms into phosphates. Corrosion then proceeds to Stage II where the rate decreases because of increase of concentration of glass components in the water. The decrease is due to a combination of decrease of driving force of extraction of glass species into solution and increase of backward transport of these species to the glass surface.
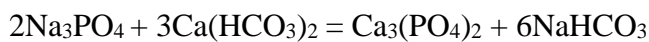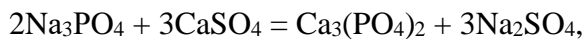
Diffusion controlled dissolution of network modifiers and/or radionuclides during Stage I and Stage II normally follow mathematically a square root of the test duration, while other radionuclides are solubility limited, entrapped in the gel layer, or complexed in secondary alteration phases that form on the glass from the leachate solution.

3

Stage III is not necessarily characteristic for all types of glasses and is characterised by a resumption of alteration with dissolution rate reaccelerated to a rate characteristic to initial corrosion rate. This is a poorly understood process which is associated with formation of specific phases on the glass surface [22, 35-38]. Note that processes characteristic to Stage III were never studied in detail for NAP glasses.

Non-uniform dissolution of glass typically seen in long-term studies [39, 40] results in a loose surface structure which trap both dissolved and non-soluble species, that are formed a result of interaction of leaching products with ground water species, backfilling materials and corrosion products. Both transport and chemical reactions occur in the surface layer. These result in a changing structure of the layer.
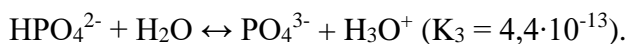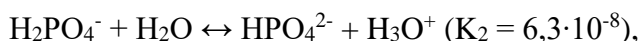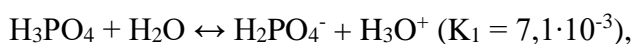
The hydrolysis of NAP glass can cause saturation of water with following compounds: [41, 42]: H_3PO_4, NaH_2PO_4, Na_2HPO_4, $Al(OH)_3$ ($Al_2O_3 \times nH_2O$), $NaAlO_2$, $Fe(OH)_2$ (Fe_2O_3 x nH_2O), $FePO_4$. Additionally, due to the contact with host rock the water can become saturated with silicic acids H_2SiO_3, H_4SiO_4 and their salts as well as with cations of Ca, Na and Mg. These can form on interaction with hydrolysis products the whole range of compounds: $CaHPO_4$, $Ca(H_2PO_4)_2$, $Ca_3(PO_4)_2$, $Ca_5(PO_4)_3OH$, $Mg_3(PO_4)_2$, $CaAl_2Si_2O_8$, $Na(AlSi_3O_8)$, $Al_2(Si_2O_5)(OH)_4$ and others which enter in the composition of surface layer.

Formation of surface layer is mainly determined by the transition into the aqueous phase of phosphate-ion in form of orthophosphoric acid and sodium orthophosphates. The latter interacts in the aqueous phase with Ca and Mg salts: $Ca(HCO_3)_2$, $Mg(HCO_3)_2$, $CaSO_4$, - for example:

$$2Na_3PO_4 + 3CaSO_4 = Ca_3(PO_4)_2 + 3Na_2SO_4,$$

$$2Na_3PO_4 + 3Ca(HCO_3)_2 = Ca_3(PO_4)_2 + 6NaHCO_3$$

Corrosion of glass is described using kinetic equations which account for the transport of each of species e.g.: H_3PO_4, Na_3PO_4, $Ca(HCO_3)_2$, $CaSO_4$, $MgSO_4$, $Mg(HCO_3)_2$. Yield of dissolved glass components is described using diffusion equations through the corrosion layer. The growth rate of layer is determined by the rate of glass dissolution and rate of precipitation of non-dissolved reaction products as well as by the rate of accumulation of hydrolysis products in the layer. Therefore first of all it is necessary to account for following products: $Ca_3(PO_4)_2$, $Mg_3(PO_4)_2$, $Al(OH)_3$, Fe_2O_3 nH_2O, $FePO_4$.

It is well known [43, 44] that orthophosphoric acid dissociates in water:

$$H_3PO_4 + H_2O \leftrightarrow H_2PO_4^- + H_3O^+ \quad (K_1 = 7,1 \cdot 10^{-3}),$$

$$H_2PO_4^- + H_2O \leftrightarrow HPO_4^{2-} + H_3O^+ \quad (K_2 = 6,3 \cdot 10^{-8}),$$

$$HPO_4^{2-} + H_2O \leftrightarrow PO_4^{3-} + H_3O^+ \quad (K_3 = 4,4 \cdot 10^{-13}).$$

Accounting for dissociation constants one can conclude that dihydrogenphosphate ions $H_2PO_4^-$ in water are significantly more abundant compared with monohydrogenphosphate ions HPO_4^{2-} and phosphate ions PO_4^{3-}. Acids form a series of salts for example NaH_2PO_4, Na_2HPO_4 and Na_3PO_4. The composition of salts depends on pH of solution. Soluble dihydrogenphosphates (such as NaH_2PO_4) yields weakly acidic solutions with pH~5. This occurs because the reaction:

$$H_2PO_4^- \rightarrow HPO_4^{2-} + H^+$$

is dominant above the reaction:

$$H_2PO_4^- + H_2O \rightarrow H_3PO_4 + OH$$
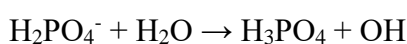
Sodium monohydrogenphosphate Na_2HPO_4 yields a weak alkali solution with pH~9 because the reaction:

$$HPO_4^{2-} + H_2O \rightarrow H_2PO_4^- + OH^-$$
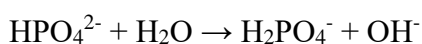
Prevails above the reaction:

$HPO_4^{2-} \rightarrow PO_4^{3-} + H^+$
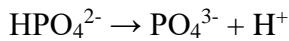
Orthophosphates such as H_3PO_4 form in strong alkali solutions with pH~12 when hydrolysis partly occurs via:

$PO_4^{3-} + H_2O \rightarrow HPO_4^{2-} + OH^-$
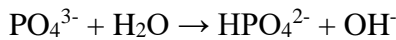
1% sodium salt solutions are characterised by following values of pH: $Na_3PO_4 = 11.8$; $Na_2HPO_4 = 4.4$; $NaH_2PO_4 = 4.4$; and $H_3PO_4 = 2.1$. Mixtures which contain ions of mono- and di-hydrogenphosphates have the pH within 6 to 8.

Therefore in alkali solutions (pH > 6) ions of PO_4^{3-} and HPO_4^{2-} form which is significant as ground waters are usually reducing.

The number of orthophosphate compounds is large e.g. the system Na_2O-P_2O_5-H_2O only includes at least 15 salts such as $Na_3PO_4 \cdot 12H_2O$, $Na_2HPO_4 \cdot 2H_2O$ and $NaH_2PO_4 \cdot 2H_2O$. These salts dissolve in water incongruently. Crystalline structures of orthophosphates revealed tetrahedral positions of oxygen atoms around phosphorus ion.

Earth alkali phosphates ususally disolve in water much worse compared alkali phosphates. For example these are $Mg(H_2PO_4)_2$; $Mg(H_2PO_4)_2 \cdot 2H_2O$; $Mg(H_2PO_4)_2 \cdot 4H_2O$; $MgHPO_4 \cdot 3H_2O$; $Mg_3(PO_4)_2$; $Mg_3(PO_4)_2 \cdot 8H_2O$; $Mg_3(PO_4)_2 \cdot 22H_2O$. Crystalline precipitates of magnesium hexa hydrogenphosphate form on adding various salts of magnesium to weakly alkali or neutral solutions. Calcium orthophosphates can play an important role in ground waters. Among them apatite is distinguished as a natural source of phosphorus. Compounds of the system CaO - P_2O_5 - H_2O are shown in the Table 1.

Table 1. CaO - P_2O_5 - H_2O compounds.

$Ca(H_2PO_4)_2$	Monocalcium phosphate
$Ca(H_2PO_4)_2 \cdot 2H_2O$	Monocalcium phosphate monohydrate
$CaHPO_4$	monetite
$CaHPO_4 \cdot 0.5H_2O$	dicalcium phosphate hemihydrate
$CaHPO_4 \cdot 2H_2O$	brushite
α-$Ca_3(PO_4)_2$	α-tricalcium phosphate
β- $Ca_3(PO_4)_2$	whitlokite
$Ca_{10}(PO_4)_6(OH)_2$	hydroxyapatite (hydroxylapatite)
$Ca_2PO_4(OH) \cdot 2H_2O$	hydroxyspodiozite
$Ca_8H_2(PO_4)_6 \cdot 5H_2O$	octacalciumphosphate
$Ca_3(PO_4)_2CaO$	tetracalciumphosphate

All these salts exept calcium monophosphate are poorly soluble and reactions with them are slow. Solubility of calcium phosphates depends on solution pH. In neutral and alkali solutions calcium phosphate salts are aligned following the order:

hydroxyapatite > whitlokite > octacalciumphosphate > monetite > $Ca(H_2PO_4)_2 \cdot H_2O$.

However monetite and brushite are the most stable (least soluble) phases at pH < 4.8.

Hydroxyapatite (or hydroxylapatite) $Ca_{10}(PO_4)_6(OH)_2$, or $3Ca_3(PO_4)_2 \cdot Ca(OH)_2$ is the most important member of a large class of compounds with generic formula $M_{10}(XO_4)_6Z_2$ (where M = metal, H_3O^+; X = P, As, Si, Ge, Cr; Z = OH, F, Cl, Br$^-$, CO_3^-, etc.). All apatite compounds have a hexagonal crystalline structure. Hydroapatites generically are non-stoichiometric characterised by ratio Ca/P within the range from 1.3 to 2.0 although the ideal formula has this ratio Ca/P =

1.67. These substances can include $CaHPO_4 \cdot 2H_2O$ or $Ca(OH)_2$, however in many cases the non-stoichiometry appears because of vacancies or substitutions in the crystalline structure or on the surface. Hydroapatite of almost ideal composition can be formed on adding calcium hydroxide into diluted phosphoric acid. Crystals precipitated in form of hexagonal plates have typical sizes ~500 Å and a large specific surface ~100 m^2/g.

Phosphoric acid readily interacts with iron (steel), aluminium, zinc, magnesium, lead. Nickel and copper are quite stable in the acid whereas zirconium, tantalum, silver, and platinum do not interact with acid. Interaction with acid depends on temperature, concentration and impurities. Traces of some organics can have inhibiting action. Phosphoric acid in a wet soil forms polymeric iron- and alumina-phosphates which cement the clayey particle of soil. Iron phosphate can form on interaction of waste containers corrosion products with ground waters.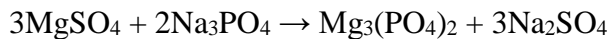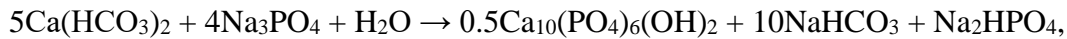 Following Fe(II)-phosphates are known: $Fe_3(PO_4)_2$, $Fe_3(PO_4)_2 \cdot 4H_2O$ (ludlamite), $Fe_3(PO_4)_2 \cdot 8H_2O$ (vivianite). Fe(III)-phosphates are: $FePO_4$ and $FePO_4 \cdot 2H_2O$ (strengite). Fe(III) salts are isotructural to aluminium salts. Acidic iron phosphates are: $FeHPO_4$; $FeHPO_4 \cdot H_2O$; $FeHPO_4 \cdot 2H_2O$; $Fe(H_2PO_4)_2$; $Fe(H_2PO_4)_2 \cdot 2H_2$ and $Fe(H_2PO_4)_3$.

$FeHPO_4$ and $Fe(H_2PO_4)_2$ in form of films form on the surface of iron and steel in diluted orthophosphoric acid. Such films act as protectors of corrosion and have a good adhesion. The chemistry of the interaction is complex and generically can be written as:

$$Fe + 2H_3PO_4 \rightarrow Fe(H_2PO_4)_2 + H_2$$
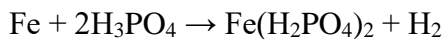
Orthophosphoric acid which is used in practice for iron (steel) passivation contains Zn^{2+} or Mn^{2+} cations the phosphates of which enter into the structure of protective films.

Vivianite belongs to the group of isomorph minerals with generic formula $A_3(XO_4)_2 \cdot 8H_2O$ (where A = Mg, Zn, Ni, Co, Fe; X = P, As). Therefore container corrosion products can act as inhibitors of NAP glass dissolution. One can note that non-soluble phosphates can form on interaction with water hardness species:

$$5Ca(HCO_3)_2 + 4Na_3PO_4 + H_2O \rightarrow 0.5Ca_{10}(PO_4)_6(OH)_2 + 10NaHCO_3 + Na_2HPO_4,$$

$$3MgSO_4 + 2Na_3PO_4 \rightarrow Mg_3(PO_4)_2 + 3Na_2SO_4$$

3. The mathematical model

We consider the following model situation (Fig. 3): flat NAP glass surface contacts ground water through a corrosion layer of thickness δ (which at t=0 is absent δ=0).
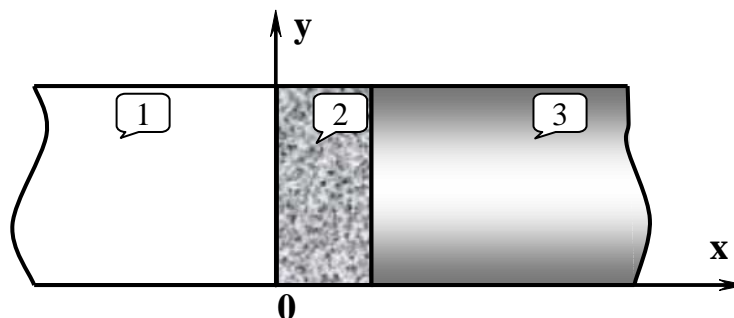

Fig. 3. Schematic of glass corrosion: 1 – water solution, 2 – corrosion layer, 3 – glass.

The model envisages the following processes:

1) Dissolution (leaching) of NAP glass network;

2) Hydrolysis products diffusion through corrosion layer;

3) Accumulation of corrosion products in the solution (and reactions among solution species) or yield of these products on water exchange.

Radioactive species (as well as others impurities) can pass into the solution and further involved in several processes: diffusion through the surface layer, immobilisation on the glass surface or in the layer. It is assumed that the diffusion coefficients of hydrolysis products, radioactive species and impurities do not change with time.

We introduce the notations: C – phosphate ions concentration in solution including the corrosion layer,; C_O – phosphate ions concentration in the NAP glass; $\delta(t)$ – layer thickness; D - phosphate ion diffusion coefficient in the corrosion layer (apparently D is close to diffusion coefficient in the water). Assuming equilibrium between phosphate ions in the solution and on the glass surface one can write the simplest model for corrosion layer growth:

$$D(\partial^2 C / \partial x^2) = \partial C / \partial t \tag{1}$$

$$C_O(\partial \delta / \partial t) = D(\partial C / \partial x) \big|_{x=\delta(t)} \tag{2}$$

The concentration in the solution out of corrosion layer is determined by water exchange rate, noting it as $C_j(t)$ one can write the boundary conditions at x = 0 and at x=$\delta(t)$:

$$C \big|_{x=0} = C_j(t) \tag{3}$$

$$C \big|_{x=\delta} = C_S \tag{4}$$

where C_s – is the concentration of saturated solution (x axis position in Fig. 3).

The exact solution of equations set (1) - (4) is not known particularly for arbitrary $C_j(t)$. However within some assumptions one can find approximate solutions. For processes that occur (see equations (1) and (2)) we have two characteristic times:

$$\tau_1 = \delta^2 / D, \text{ and } \tau_2 = (C_O / C)\delta^2 / D \tag{5}$$

Accounting that $C_0 \gg C$ we have $\tau_1 \ll \tau_2$. For small thicknesses δ we have the following inequalities for the time t:

$$\tau_1 \ll t \ll \tau_2 \tag{6}$$

In this case we can consider the stationary diffusion of species through a constant thickness layer which slowly changes. If $C_j=const(t)$ then we can analytically find the solution for $\delta(t)$:

$$\delta(t) = \left[2(C_S - C_j)Dt / C_O \right]^{1/2} \tag{7}$$

Analytical solution is possible also for $C_j(t)$ if the characteristic time of $C_j(t)$ changes is high compared t:

$$\delta(t) = \left\{ (2D/C_O) \int_0^t dt \left[C_S - C_j(t) \right] \right\}^{1/2} \tag{8}$$

Equation (7) shows that the thickness of corrosion layer increases with time as $t^{1/2}$. If $C_j=C_S$ then the layer does not grow. Here it is necessary to account for conditions of ensuring layer growth in conditions of saturation.

It is worth to note that δ - is the thickness of glass which corroded. Here δ is equalised to the thickness of corrosion layer although they may differ. If the corrosion layer swells and its thickness is larger than the thickness of corroded glass then we can define an expansion coefficient to account for that. Following (7) if we multiply the diffusion coefficient to the second power of that expansion coefficient then we obtain a new effective diffusion coefficient so keeping all equations unchanged. Therefore we will further consider δ as the thickness of corrosion layer on the NAP glass.

The yield of NAP glass components with small concentrations considered as impurities is determined by the glass dissolution rate which is found from equations (1) - (4) (and thus by equation (7)) and by the rate of precipitation of those components on the NAP glass surface and within the corrosion layer (see Fi. 3 – the boundary between 2 and 3). Mathematically the situation is described by following:

1) Impurity diffusion through the layer with the capture of the impurities in the layer

$$D_n \partial b^2 / \partial x^2 - Kb = \frac{\partial b}{\partial t} \tag{9}$$

where b - the concentration of impurities in the solution (including the inside of corrosion layer), D_n - diffusion coefficient of impurities through the surface layer, K - coefficient of the impurity trapping in the surface layer.

2) Boundary condition on the boundary of the intact glass and corrosion layer:

$$D_n \partial b / \partial x \big|_{x=\delta(t)} = \varpi_n C_O [\partial \delta(t) / \partial t] - P(b - b_S) \tag{10}$$

where ϖ_n – the molar fraction of impurities (including radionuclides) in the glass (relatively to the content of phosphate-ion); b_S - the concentration of saturated (for impurities) solution, P – kinetic constant; for $\delta(t)$ we use equations (7) or (8);

3) Boundary condition for x = 0:

$$b \big|_{x=0} = b_j(t) \tag{11}$$

For impurities one can accept $b_j(t)=0$. (12)

In general, the problem [see. Equations (9) - (11)] is solved numerically, but in the case of quasi-stationary diffusion conditions for (12) we can write the approximate solution:

$$b = b_1 sh\lambda x, \quad \lambda = (KD_n^{-1})^{1/2} \tag{13}$$

$$b_1 = (\varpi C_O \partial \delta / \partial t + Pb_S)/(Psh[\lambda\delta] + D_n \lambda sh[\lambda\delta]) \tag{14}$$

Impurity flux is given by formula:

$$j = D_n \partial b / \partial x \big|_{x=0} = D_n \lambda b_1 \tag{15}$$

In the absence of capturing impurities in the corrosion layer (K = 0) formulas are simplified:

$$b = b \big|_{x=\delta} x/\delta, b_1 \big|_{x=\delta} = \delta / D_n (\varpi_n C_O \partial \delta / \partial t + Pb_S)/(1 + P\delta / D_n) \tag{16}$$

It is interesting the behaviour of $b \big|_{x=\delta}$ in the limits when t→0 and t→∞:

t→0, $\quad b \big|_{x=\delta} \to \varpi_n D(C_S - C_j)D_n^{-1}$;

t→∞, $\quad b \big|_{x=\delta} \to b_S$

Thus, the impurity concentration becomes close to a saturated solution within the corrosion layer in the vicinity of the glass surface.

4. Leaching of NAP glass components

The fission fragments and actinides as well as NAO glass components may be exposed to water by two mechanisms. The first involves a very slow diffusion component in the glass. Another mechanism is decisive: the dissolution of the glass matrix, and is accompanied by the release of the release of the individual components (see e.g. the reference [JNM]). Glass impurities including radionuclides pass into solution simultaneously with the components. However but their fate

is determined by several processes: diffusion through the surface corrosion layer, capturing by the glass surface and corrosion layer, and chemical reactions with components of the solution. Mathematically, the above processes are described by the equations (9) - (12) or limit cases (13) - (16). Note the condition (10), setting the rate of the impurity components formation due to the hydrolysis of the glass.

It is important to find the maximum release rate of the impurity in the water - the yield equivalent to the speed of dissolution of glass:

$$j_{ko} = C_{ok} \partial \delta(t) / \partial t \qquad (17)$$

Here C_{ok} – concentration of k-th component of glass. Equation (17) gives the maximum specie yield without any account of capturing processes on the glass surface and within the corrosion layer. It is significant that in the limit (see. Equation (17)) the leaching rate of all components is the same.

$$V_k = j_{ko} / C_{ok} = \partial \delta(t) / \partial t = V_o \qquad (18)$$

and coincides with the growth rate of corrosion layer.

The solution of equations (13) - (16) corresponds to the condition (12), that is, to a state where there is no any admixture in the aqueous solution in contact with the surface layer. In the case of conditions (11), that is when an impurity is present in the solution, then yield is found from:

$$b_k = b_{jk} + b_k sh\lambda_k x , \qquad (19)$$

$$b_k = [j_k + P_k(b_{sk} - b_{jk})] / [P_k sh\lambda_k \delta + D_k \lambda_k ch\lambda_k \delta], \qquad (20)$$

$$\lambda_k = (K_k D_k^{-1})^{1/2} \qquad (21)$$

where the flux j_k for the k-th impurity is taken from (17), D_k- impurity diffusion coefficient in the corrosion layer. Using these formulas, it is easy to find the flux of components from the glass surface (compare with formula (15)):

$$j_k = b_k \lambda_k D_k \qquad (22)$$

This equation describes leaching of impurities which are captured by the corrosion layer and glass surface. We can examine that equation for $K_k \rightarrow 0$, $P_k \rightarrow 0$ when we have

$$j_k \rightarrow j_{ko} , \qquad (23)$$

that was expected to occur.

It is pointed out that due to the glass surface capturing of impurities generally the concentration of components in the glass (more precisely, on the surface of the glass) will vary over time - a fact that is not included in the formulas above.

This can be done when considering the initial leaching stage. In this connection, we can write the formula for j_k when $P_k=0$, i.e. when there is no flow of impurities from the solution to the glass surface :

$$j_k = (j_{ko} / ch\lambda_k \delta), \qquad (24)$$

where the denominator $ch\lambda_k \delta$ is always greater than one, therefore j_{ko} is always greater than j_k, due to absorption of components inside the corrosion layer. To check the formula (24) let us make the transition $K_k \rightarrow 0$ when we obtain $j_k \rightarrow j_{ko}$.

5. Leaching of NAP glass impurities and radionuclides

The leaching rate of impurities which do not bind in the corrosion layer and on the surface of undisturbed glass is defined by the formula (18). Account of specie capturing in the layer decreases the yield following the equation:

$$V_k = V_o / ch\lambda_k \delta . \tag{25}$$

Important to note that both V_k and V_o do not depend on k-th component contents in the glass although some dependence might be expected die to accumulation of impurities which is not analysed here.

Equations (18) and (25) of the leaching rate of the glass components in underground water indicate that it is determined by glass corrosion rate, i.e. on the rate at which the corrosion layer grows and on corrosion depth of glass.

The specifics of each of the components is found in the formulas through constants λ_k. Its physical sense is easiest to understand if we define characteristic value with the dimension of length

$$L_k = \lambda_k^{-1} = \sqrt{(D_k / K_k)} \tag{26}$$

The length L_k increases with increasing impurity mobility and decreases with increasing absorption of impurities in the surface layer. It determines the scale value (corrosion thickness) in which the absorption is set or not. Graphs illustrate this for the initial stage of corrosion, when formula (7) is correct. In the absence of absorption we have:

$$V_k = V_o = \left[\frac{D(C_S - C_j)C_O}{2t} \right]^{1/2} \tag{27}$$

Fig. 4 shows the plots of $V_o(t)$ and $\delta(t)$, where the dependences $\delta(t)$ proportional to $t^{1/2}$ and V_k proportional to $t^{-1/2}$ look diffusion-like which in many cases is treated as an indication on diffusion rather than glass corrosion.
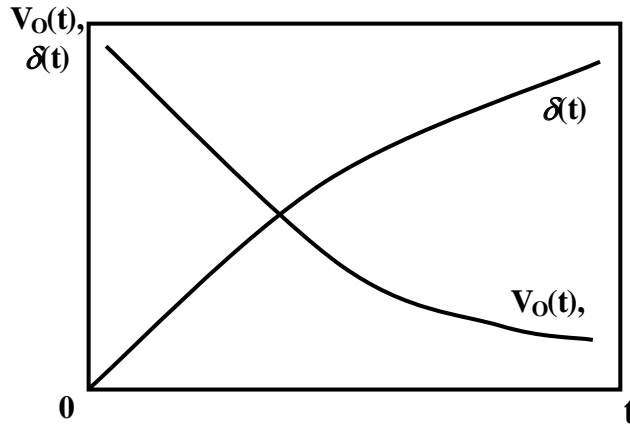
Fig. 4. Schematic of NAP glass corrosion layer growth rate $V_o(t)$ and its corrosion layer thickness $\delta(t)$ with time.

Fig. 4 shows that the leaching rate decreases with time (proportionally to $t^{1/2}$) even if there is no absorption of the impurity in the corrosion layer. If this absorption is available, leaching decreases even faster, which is especially noticeable [see formula (25)] with an increase in corrosion layer thickness (Fig. 5).
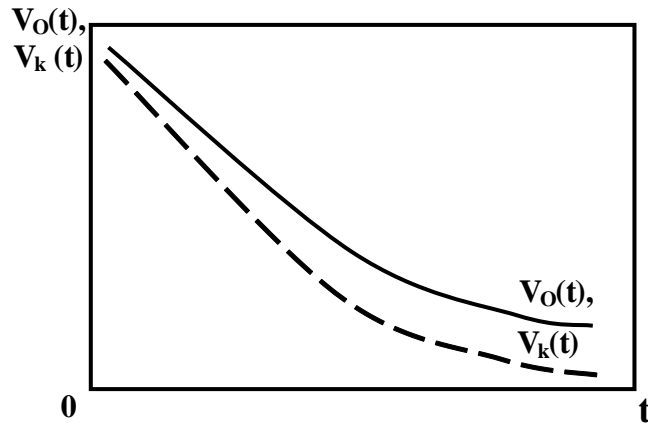
Fig. 5. Schematic of NAP glass corrosion layer growth rate $V_o(t)$ and k-th specie leaching rate $V_k(t)$ with time.

6. NAP glass dissolution on solution saturation

According to formula (7) the glass hydrolysis stops on achieving solution saturation by phosphate ions. For multi-component structures, which include glass, such a statement is not quite correct: the dissolution of the glass continues even if contacting solution saturation occurs on the main structure-forming component. Apparently, this behaviour is ensured because no saturation occurs of other components of the solid matrix, which leads to their dissolution, degradation on the solid matrix surface with a corresponding primary structure-forming components exit.

We describe corrosion of NAP glass in an aqueous phase with the possibility of hydrolysis in conditions when phosphate ion concentrations achieve saturation levels. For this purpose we add to the diffusion flow a flux at the boundary of corrosion layer with glass (the boundary between mediums 2 and 3 in Fig. 3). Diffusion of phosphate ions through the corrosion layer is still described by the diffusion equation (1). Taking into account the additional flow the condition on the boundary separating the corrosion layer and glass can be written as:

$$C_O \partial \delta / \partial t = D \partial C / \partial x \big|_{x=\delta(t)} + j_\infty \qquad (28)$$

where j_∞ - phosphate ion flux on dissolution of NAP glass by the aqueous solution saturated with phosphate ions. The value j_∞ is introduced phenomenologically. The concentration of species in the solution out of corrosion layer is determined by the rate of water exchange. Designate that concentration as $C_j(t)$, then we can write:

$$C \big|_{x=0} = C_j(t) \qquad (29)$$

When $x = \delta(t)$ the condition of solution saturation is valid

$$C \big|_{x=\delta(t)} = C_S, \qquad (30)$$

where C_S - the saturation concentration of phosphate ions at the temperature of underground disposal.

The analytical solution of the nonlinear problem (1), (28) - (30) is obtained under the assumption of a stationary diffusion. Equation (28) is transformed to:

$$C_O \partial \delta / \partial t = D(C_S - C_j)\delta(t) + j_\infty \qquad (31)$$

Equation (31) can be easily integrated, assuming that the temperature of disposal does not vary (and therefore D, C_S and j_∞ are unchanged) whereas the concentration of phosphate ions in the solution is stabilised [C_j = const(t)];

$$\delta - \left[D(C_S - C_j) / j_\infty \right] \ln \left[1 + j_\infty \delta / D(C_S - C_j) \right] = j_\infty t / C_O \qquad (32)$$

11

Here, the constant of integration is selected so that so that we have δ→0 when t→0.

It is interesting to consider the limiting cases for unsaturated phosphate ion and a saturated solution that is determined by the dimensionless parameter:

$$S = j_\infty \delta(t) / D(C_S - C_j) \tag{33}$$

If the solution is unsaturated (S<<1) then from equation (32) follows formula (7). In the opposite case (S>>1) of hydrolysis in saturated solutions the corrosion layer grows at a constant rate:

$$\delta(t) = j_\infty t / C_O \tag{34}$$

Equation (31) for the corrosion layer thickness is very convenient for studying the stability of the growth of flat corrosion layer. Let the time t_0 corrosion flat surface of the glass has a value $\delta(t_0)$. Assume at this point that a perturbation corrosion front, i.e. the thickness of the corrosion layer at different points on the surface is different from $\delta(t_0)$:

$$\delta(x, y, z) = \delta_O + \Delta,$$

where y, z - coordinates on the flat surface of the glass; it is assumed that the perturbation is small $|\Delta| << \delta(t_0)$. The question arises on how a deviation from the plane front will be developed with time $t > t_0$?

Designate $\delta(y, z, t) = \delta(t_O) + \Delta(y, z, t)$. For small perturbations Δ from the equation (31) we get:

$$C_O \partial \Delta / \partial t = -D(C_S - C_j) / \delta^2(t_O) \Delta \tag{35}$$

The solution of this equation is a decaying exponent:

$$\Delta(y, z, t) = \Delta_O \left\{ (y, z, t_O) \exp\left[-\lambda(t - t_O) \right] \right\} \tag{36}$$

where

$$\lambda = D(C_S - C_j) / C_O \delta^2(t_O) \tag{37}$$

This means that the flat corrosion front of homogeneous glass is stable: all disturbances of this front damp and the thicker layer of corrosion, the faster perturbations smooth over.

In conclusion, we note that the use of equations (31) to describe the disturbances suggests that disturbances are long-wave with a wavelength much longer than δ(t), while short-wave perturbations are smoothed out quickly - within a diffusion times.

7. Application of mathematical model to experiment

The yield of NAP glass components is determined by the rate of penetration of the corrosion inside the glass, so the experimental determination of the corrosion rate is very important. It is easy to determine the corrosion rate using standard short term experiments. According to the simulation results (see formula (18)) the maximum rate of leaching matches the speed of corrosion layer growth. In accordance with the above, to determine the corrosion rate of the glass matrix from experimental leaching data it is necessary to select the element with maximum value of the leaching rate. For the NAP glass this is caesium.

Transform formulas for the purposes of processing experimental data. If we write m_k - leaching rate of k-th the element, then

$$m_k = \rho V_k \tag{38}$$

where $\rho = (2,6 - 2,7)$ g/cm^3 – glass density. In accordance with the formula (24) we have:

$$m_k = \rho(d\delta / dt) / ch\lambda_k \delta \tag{39}$$

This means that it is always the inequality

$$m_k \leq \rho(d\delta / dt) \tag{40}$$

Thus, choosing from a number of experimental m_k the item with a maximum value we find mass corrosion rate:

$$\rho(\mathrm{d}\delta / \mathrm{dt}) = m_{k\,max} \tag{41}$$

This formula is easy to use for the treatment of experimental data.

We introduce here the following designations:

$$B = t^{1/2} m_{kmax} / 2^{1/2} \tag{42}$$

$$M = t m_{kmax} \tag{43}$$

If we compare the formula (7), (18) and (42), we see that B in conditions described (see formula (7)) in experiments becomes constant, which is well illustrated by the last two columns in the table.

Accordingly, the mass value M determines the mass of glass involved in the corrosion process (this mass, of course, refers to the unit of surface area). As before δ denotes the thickness of the corrosion layer, defined by the formula:

$$\delta = M/\rho \tag{44}$$

From [10, 32] we can get data given below in Table 2 for caesium leaching from NAP glass in deionised water at 20°C.

Table 2. Processing of experimental data on caesium leaching, $m_{kmax} = 4.1 \times 10^{-6}$ g/cm^2·d

parameter	Time, days			
	1	8	15	29
m_y, 10^{-6} g/cm^2·d	3.3	4.1	1.7	1.1
B, 10^{-5} g/cm^2·d$^{1/2}$	-	0.82	1.1	1.6
M, 10^{-5} g/cm^2	-	3.3	6.2	12
δ, μm	-	0.13	0.24	0.46

For other temperatures we can construct a similar table using the data where one can find the activation energy of the corrosion process. According to (7), (28), (41) and (42) the relation occurs

$$(B/\rho)^2 = C_S D/C_O \tag{45}$$

For the product $C_S D$ (value of the saturation concentration of phosphate ion in solution multiplied to its diffusion coefficient in solution) is natural to expect the activation behaviour:

$$C_S D = (C_S D)_O \exp(-T_a/T), \tag{46}$$

where T_a – activation temperature, T – temperature in Kelvin degrees. According to equations (45) and (46) we can use the following formula for calculating the activation temperature

$$T_a = 2(\ln B_2 - \ln B_1)/(T_1^{-1} - T_2^{-1}) \tag{47}$$

Using evaluation $m_{kmax} = (2,3 \pm 0,1) \times 10^{-5}$ g/cm^2·d for NAP glass in deionised water at 120°C on the basis of experimental data from [10] we get: $T_a = (4,0 \pm 0,4) \, 10^3$ K, respectively, the activation heat (energy) is: $Q_a = R T_a = (33 \pm 3)$ kJ/mol.

According to the formulas (46) and (47) for B the temperature and the activation energy for the corrosion rate corresponds to half of the values T_a and Q_a:

$T_B = T_a/2 = (2,0 \pm 0,2) \, 10^3 \, K$,

$Q_B = Q_a/2 = (17\pm2) \, kJ/mol$ (48)

For B the equation is valid $B = B_o \exp(-T_B/T)$, where $B_o = 0,44 \cdot 10^{-1} \, g/cm^2 day^{1/2}$ with errors in determining B retained in determination of T_B.

8. Conclusions

In conditions of disposal of radioactive waste the radionuclides yield from NAP glasses is determined by their transport from the matrix through the surface layer into the groundwater and the subsequent transfer by these waters. Formation of the surface layer is due to the dissolution of the glass network components and the formation of insoluble compounds from chemical reactions between the components of the solution supplied by the glass dissolution, the geological environment and the corrosion products of packages of vitrified waste. Radionuclides escaping from the NAP glass can also react with the components of the solution, forming the precipitated products, or they can be captured by glass corrosion insoluble components (for example, by adsorption). Thus, the problem of leaching of radionuclide from the glass blocks cannot be understood and described excluding glass corrosion processes.

The mathematical model of NAP glass aqueous corrosion takes into account glass dissolution process due to hydrolysis, formation of surface corrosion layer, specie diffusion via the corrosion layer and the chemical reactions in solution. We have found approximate analytical solutions of growth rate of corrosion layer and of glass components component leaching rates. It has been accounted that a non-zero solubility of glass exists in solutions saturated with phosphate ions. In the initial stages of dissolution the yield of phosphate ion into the groundwater solution is similar to the diffusion that is proportional to the square root of time. However, the dependence on time changes as the process evolves, and finally the total output increases linearly with time. We have proved the stability of the flat front of corrosion layer growth with time. The mathematical model was used for the analysis of experimental data.

To assess the corrosion of NAP glass and specie leaching rates one can use the following formulae, and experimental factors:

1) Glass corrosion depth: $\delta(t) = B(2t)^{1/2}/\rho$;

2) Leaching of the individual elements (without normalisation on the content of the element in the matrix) $m_k \le C_{ok}B/(t^{1/2} \, 100\%)$;

3) $B = B_o\exp(-Q_B/RT)$, where t - time (days), $C_{ок}$ – mass content of к-th element in the glass, %, $\rho = 2,6 - 2,7 \, g/cm^3$ – glass density, $B_0 = 0,44 \times 10^{-1} \, g/cm^2 \cdot d^{1/2}$ (at temperatures 20 - 120 °C), $Q_B = RT_B = (17 \pm 2) \, kJ/mol$, $T_B = (2,0 \pm 0,2) \, 10^3 \, K$.

The thickness of corrosion layer can be estimated using the depth of glass corrosion δ excluding the layer formed by the interaction of glass products of hydrolysis with mineral components of the underground water. Formulas given above enable calculation of the maximum rate of corrosion of glass, provided as a result of the water exchange there is no phosphate ion present. Thus, even at 120 °C for 10 thousand years the depth of surface corrosion phosphate glass is approximately 0.3 cm. It should be borne in mind that as shown by evaluation the disposal temperature is equalized with the ambient temperature of the rock during the first 200 years (when heat-releasing short-lived fission products have been fully decayed). This means that the rate of release of the different components of the glass could essentially increase only if the glass-water contact surface has been increased due to mechanical failure of the glass [45, 46]. Additional impact may have the radiation damage due to self-irradiation of NAP glass in the disposal environment [8, 9, 47, 48].

References

1. B.L. Cohen. High-level radioactive waste from light-water reactors. Rev. Mod. Phys., **49** (1) (1977) 1- 20.
2. K.L. Nash, G.J. Lumetta. Advanced Separation Techniques for Nuclear Fuel Reprocessing and Radioactive Waste Treatment. Woodhead, Cambridge, 492 p. (2011).
3. I.W. Donald. Waste Immobilisation in Glass and Ceramic Based Hosts. Wiley, Chichester (2010).
4. M.I. Ojovan, W.E. Lee. An Introduction to Nuclear Waste Immobilisation, Second Edition, Elsevier, Amsterdam, 362 p. (2014).
5. W. E. Lee, M.I. Ojovan, C.M. Jantzen (Eds.). Radioactive waste management and contaminated site clean-up: Processes, technologies and international experience, Woodhead, Cambridge, 924 p. (2013).
6. C.M. Jantzen. Historical development of glass and ceramic waste forms for high level radioactive waste. In: Ojovan M. Handbook of Advanced Radioactive Waste Conditioning Technologies. Woodhead, Cambridge. 159-172 (2011).
7. C.M. Jantzen. (2011). Development of glass matrices for HLW radioactive wastes. In: Ojovan M. Handbook of Advanced Radioactive Waste Conditioning Technologies. Woodhead, Cambridge. 230-292 (2011).
8. M.I. Ojovan, W.E. Lee. Glassy wasteforms for nuclear waste immobilisation. Metallurgical and Materials Transactions A, **42** (4) (2011)., 837-851
9. M.I. Ojovan, W.E. Lee. New Developments in Glassy Nuclear Wasteforms, Nova, New York, 131p (2007).
10. A.A. Vashman, A.V. Demine, N.V. Krylova, V.V. Kushnikov, Yu.I. Matyunin, P.P. Poluektov, A.S. Polyakov, E.G. Teterin. Phosphate Glasses with Radioactive Waste. CNIIatominform, Moscow, 172 p. (1997).
11. D. Caurant, P. Loiseau, O. Majérus, V. Aubin Chevaldonnet, I. Bardez, A. Quintas. Glasses, Glass-Ceramics and Ceramics for Immobilization of Highly Radioactive Nuclear Wastes. Nova, New York (2009).
12. R.A. Robbins, M.I. Ojovan. Vitreous Materials for Nuclear Waste Immobilisation and IAEA Support Activities. Mater. Res. Soc. Symp. Proc., in press (2016).
13. IAEA. Radiation Protection and Safety of Radiation Sources: International Basic Safety Standards. General Safety Requirements Part 3, IAEA Safety Standards Series No. GSR Part 3, IAEA, Vienna (2014).
14. IAEA. (2009). Classification of Radioactive Waste. General Safety Guide GSG-1. IAEA, Vienna.
15. IAEA. (2003). Scientific and Technical Basis for Geological Disposal of Radioactive Wastes. TRS-413. IAEA, Vienna.
16. J. Ahn, M.J. Apted. Geological Repository Systems for Safe Disposal of Spent Nuclear Fuels and Radioactive Waste. Woodhead, Cambridge, 792 p. (2010).
17. N. Chapman, C. McCombie. Principles and Standards for the Disposal of Long-lived Radioactive Wastes. Elsevier, Amsterdam, 250 p. (2003).
18. N.A. Chapman, I.G. McKinley. The Geological Disposal of Radioactive Waste. John Wiley and Sons, New York (1987).
19. S. Gin, A. Abdelouas, L.J. Criscenti, W.L. Ebert, K. Ferrand, T. Geisler, M.T. Harrison, Y. Inagaki, S. Mitsui, K.T. Mueller, J.C. Marra, C.G. Pantano, E.M. Pierce, J.V. Ryan, J.M. Shoefield, C.I. Steefel, J.D. Vienna. An international initiative on long-term behaviour of high-level nuclear waste glass. Materials Today, **16** (6) (2013) 243-248.
20. P. Van Iseghem. Corrosion issues of radioactive waste packages in geological disposal systems. In: D. Féron. Nuclear corrosion science and engineering, Woodhead, Oxford, 939-987 (2012).

21. C.M. Jantzen, K.G. Brown, J.B. Pickett. Durable glass for thousands of years. International Journal of Applied Glass Science, **1** (2010) 38-62.
22. D. Bacon, E. Pierce. Development of long-term behaviour models. In: M. Ojovan. Handbook of Advanced Radioactive Waste Conditioning Technologies, 433-454, Woodhead, Cambridge (2011).
23. D.E. Clark, C.G. Pantano, L.L. Hench. Corrosion of Glass. Books for Industry, New York, NY (1979).
24. J.E. Mendel, A. Barkatt, P.B. Macedo, C.J. Montrose, D.D. Jackson, M.J. Apted, G.L. Mcvay, W.B. White, C.G. Pantano, A.B. Harker, D.E. Clark, L.L. Hench. Final Report of the Defense High-Level Waste Leaching Mechanisms Program, PNL-5157, Pacific Northwest Laboratory, Richland, WA (1984).
25. J.K. Bates, C.R. Bradley, E.C. Buck, J.C. Cunnane, W.L. Ebert, X. Feng, J.J. Mazer, D.J. Wronkiewicz, J. Sproull, W.L. Bourcier, B.P. Mcgrail, and M.K. Altenhofen. High-Level Waste Borosilicate Glass: A Compendium of Corrosion Characteristics, DOE/EM-0177, U.S. Department of Energy, Office of Environmental Management, Washington, D.C. (1994).
26. W.L. Bourcier. Critical Review of Glass Performance Modeling, ANL-94/17, Argonne National Laboratory, Argonne, IL (1994).
27. W.L. Ebert, J.J. Mazer. Laboratory Testing of Waste Glass Aqueous Corrosion: Effects of Experimental Parameters. Mat. Res. Soc. Symp. Proc. **333** (1994) 27-40.
28. P. Van Iseghem, M. Aertsens, S. Gin, D. Deneele, B. Grambow, D. Strachan, P. Mcgrail, G. Wicks. Glamor - a Critical Evaluation of the Dissolution Mechanisms of High Level Waste Glasses in Conditions of Relevance for Geological Disposal (2007).
29. E.Y. Vernaz, J.L. Dussossoy. Current State of Knowledge of Nuclear Waste Glass Corrosion Mechanisms - the Case of R7T7 Glass. Applied Geochemistry. 13-22 (1992).
30. M. Aertsens. An Overview of Simple Basic Equations Used in HLW Glass Dissolution Modeling: Consequences for Long Term Leaching and Element Profiles. Mat. Res. Soc. Symp. Proc. **932** (2006) 401-409.
31. J.V. Ryan, W.L. Ebert, J.P. Icenhower, D.M. Strachan, C.I. Steefel, L.J. Criscenti, I.C. Bourg, R.E. Williford, K.A. Murphy, C.G. Pantano, E.M. Pierce, D.K. Shuh, G.A. Waychunas, J.C. Marra, J.D. Vienna, P. Zapol, C.M. Jantzen. Technical Program Plan for the International Technical Evaluation of Alteration Mechanisms (I-Team), PNNL-21031, Pacific Northwest National Laboratory, Richland, WA (2011).
32. N.V. Krylova, P.P. Poluektov. Properties of solidified forms of high level wastes as one of barriers in the disposal system. Atomic Energy, **78** (2) (1995) 93–99.
33. M.I. Ojovan, R.J. Hand, N.V. Ojovan, W.E. Lee. Corrosion of alkali-borosilicate waste glass K-26 in non-saturated conditions. J. Nucl. Mat. **340**(2005) 12-24.
34. M.I. Ojovan, W.E. Lee. About U(t) form of pH-dependence of glass corrosion rates at zero surface to volume ratio. Mat. Res. Soc. Symp. Proc., **1744**(2015) 9 p.
35. C.M. Jantzen, W.E. Lee, M.I. Ojovan. Radioactive waste (RAW) conditioning, immobilisation, and encapsulation processes and technologies: overview and advances. Chapter 6 in: Radioactive waste management and contaminated site clean-up: Processes, technologies and international experience. Ed. W.E. Lee, M.I. Ojovan, C.M. Jantzen. p. 171-272, Woodhead, Cambridge (2013).
36. W.L. Ebert, J.K. Bates, E.C. Buck, and C.R. Bradley. Accelerated Glass Reaction under PCT Conditions. Mat. Res. Soc. Symp. Proc. **294** (1993) 569-576.
37. A. Barkatt, S.A. Olszowka, W. Sousanpour, M.A. Adel-Hadadi, R. Adiga, A. Baraktt, G.S. Marbury, S. Li. Leach Rate Excursions in Borosilicate Glasses: Effects of Glass and Leachant Composition, Mat. Res. Soc. Symp. Proc. **212**, 65-76 (1991).
38. P. Van Iseghem, T. Amaya, Y. Suzuki, H. Yamamoto. The Role of Al_2O_3 in the Long-Term Corrosion Stability of Nuclear Waste Glasses. Journal of Nuclear Materials, **190** (1992) 269-276.

39. M.I. Ojovan, W.E. Lee, A.S. Barinov, I.V. Startceva, D.H. Bacon, B.P. McGrail, J.D. Vienna. Corrosion of low level vitrified radioactive waste in a loamy soil. Glass Technol., **47** (2) (2006) 48-55.

40. N.V. Ojovan, I. V. Startceva, A.S. Barinov, A.V. Mokhov, M.I. Ojovan, G. Moebus. Secondary phases on the surface of real vitrified radioactive waste disposed in a loamy soil. Mat. Res. Soc. Symp. Proc. **807**, 139-144 (2004).

41. Chemical encyclopaedic handbook. Ed. I.L. Knunyants. Moscow, Sovetskaya Enciclopedia, (1983).

42. Mining encyclopaedia. V.3. Moscow, Sovetskaya Enciclopedia, p. 229 (1987).

43. E.J. Griffith, A. Beeton, J.M. Spencer, D.T. Mitchell, eds. Environmental Phosphorus Handbook, John Wiley and Sons, New York-London-Sydney-Toronto (1973).

44. D.E.C. Corbridge. Phosphorus: An Outline of its Chemistry, Biochemistry and Technology. Elsevier Scientific Publishing Company, Amsterdam - Oxford - New York (1980).

45. I.A. Sobolev, M.I. Ojovan, O.G. Batykhnova, N.V. Ojovan, T.D. Scherbatova, Waste glass leaching and alteration under conditions of open site tests, Mater. Res. Soc. Symp. Proc. **465** (1997) 245–252.

46. M.I. Ojovan. Mass spectrometric evidencing on modified random network microstructure and medium range order in silicate glasses. J. Non-Cryst. Solids, **434** (2016) 71-78.

47. G. Möbus, M. Ojovan, S. Cook, J. Tsai, G. Yang. Nano-scale quasi-melting of alkali-borosilicate glasses under electron irradiation. J. Nucl. Mater., **396** (2-3) (2010) 264-271.

48. M. Chromcikova, J. Vokelova, J. Mikhalkova, M. Liska, J. Machacek, O. Gedeon, V. Sotesz. Chemical durability of gamma-irradiated glass fibrous insulation. Nuclear Technology, **193** (2016) 297-305.